MEDIATOR OF DNA DAMAGE CHECKPOINT 1 (MDC1) IS A NOVEL ESTROGEN RECEPTOR CO-REGULATOR IN INVASIVE LOBULAR CARCINOMA (ILC) OF THE BREAST

by

EVELYN KAY BORDEAUX

B.S., Seattle University, 2017

A thesis submitted to the

Faculty of the Graduate School of the

University of Colorado in partial fulfillment

of the requirements for the degree of

Masters of Science

Biomedical Basic Science Program

2020

This thesis for the Master of Science degree by

Evelyn Kay Bordeaux

has been approved for the

Biomedical Basic Science Program

by

Heide Ford, Chair

Joshua Black

Benjamin Bitler

Matthew Sikora, Advisor

Date: December 13th, 2020

Bordeaux, Evelyn Kay (M.S. Biomedical Basic Science Program)

Mediator of DNA Damage Checkpoint 1 (MDC1) is a Novel Estrogen Receptor Coregulator in Invasive Lobular Carcinoma (ILC) of the Breast

Thesis directed by Assistant Professor Matthew J. Sikora

ABSTRACT

Invasive Lobular Carcinoma (ILC) is the 2nd most common histotype of breast cancer yet is critically understudied. ~95% of ILC are estrogen receptor (ER) positive, and previous studies demonstrate the importance of estrogen in ILC etiology. However, retrospective studies show that anti-estrogens are substantially less effective in ILC than in ER+ Invasive Ductal Carcinoma (IDC). This strongly suggests that regulation of ER function is distinct in ILC. We hypothesize that this is due to an ILC-specific cohort of ER co-regulators. We performed Rapid Immunoprecipitation Mass Spectrometry of Endogenous Proteins (RIME) to determine ILC-specific ER-interacting proteins and identified Mediator of DNA Damage Checkpoint 1 (MDC1) as a novel ER co-regulator in ILC cells. ER:MDC1 interaction was confirmed by co-immunoprecipitation and proximity ligation assays (PLA); interaction was specifically observed in ILC cell lines but not IDC cell lines. Consistent with co-regulator function, MDC1 is essential for ER-driven proliferation of ILC cells. MDC1 knockdown dysregulates transcription of ER target genes in ILC cells. Moreover, RNA-seq analysis showed that in ILC cell line MDA MB 134VI, >50% of ER target genes require MDC1 for their regulation. Together, these data suggest MDC1 acts as a novel ER co-regulator in ILC that regulates ER transcriptional function to drive ILC cell proliferation and survival.

The form and content of this abstract are approved. I recommend its publication.

Approved: Matthew J. Sikora, PhD

ACKNOWLEDGMENTS

I would like to express my deep and sincere gratitude to my mentor and lab PI, Dr. Matthew Sikora, for his guidance and support throughout my time in graduate school and work on this project. As much as we may joke about how mentally taxing one-on-one meetings or "runs" are with Matt, they are incredibly valuable learning opportunities that have greatly developed my skills as a scientist and analytical thinker.

I would also like to thank all the members and rotation students of the Sikora Lab, past and present. Thank you especially to Dr. Joseph Sottnik for sharing your expertise and for your extensive work with assay development, as well as the data you have contributed to this project. Thank you to both Maddy Shackleford and Devi Rao for your enthusiastic encouragement, friendship, and lab conversations that always brought me joy throughout my workday.

Thank you to my Comprehensive Exam Committee, Drs. Heide Ford, Mair Churchill, Jennifer Richer, Joshua Black, and Benjamin Bitler, as well as my Masters Defense Committee, Drs. Heide Ford, Joshua Black, and Benjamin Bitler for their expert guidance and advice.

Special gratitude to my family, especially my parents Bob and Shelli Bordeaux, and friends, particularly Allie McMellen for being an invaluable study and writing buddy.

I particularly want to acknowledge everyone's support and encouragement in my decision to exit the PhD program. I have received excellent training and mentoring during my time in the Pharmacology PhD program and the Sikora Lab, and I will value and utilize this experience in many aspects of my career and life. It was important to me to reflect the ongoing nature of this project in the writing of my thesis, because while I am proud of the data I've collected and the conclusions I've made, my preliminary data has me excited for the future of this project is exciting and I look forward to seeing where it goes.

TABLE OF CONTENTS

INTRODUCTION

Breast cancer is the second most common cancer diagnosed among women in the United states, and in 2017 alone 250,520 new cases were diagnosed[1]. Approximately 80% of breast cancers are classified as Invasive Ductal Carcinoma (IDC). However there exist many different breast cancer subtypes that, while less common, represent a significant patient population. Invasive Lobular Carcinoma (ILC) is the second most common histological breast cancer subtype, accounting for 10-15% of all breast cancer cases[2]. ILC is a biologically distinct form of breast cancer characterized by a single-file growth pattern of tumor cells within the breast stroma[3,4]. This unique growth pattern means that ILC does not form a distinct tumor mass and as such, clinical detection by mammography is difficult. This means ILC patients are often diagnosed at older ages and later stages of cancer progression as compared IDC. Approximately 90-95% if ILC cases express estrogen receptor (ER), compared to only 60-70% of IDC cases[5]. Based on this, it would be expected that ILC patients should show greater benefit from endocrine therapy compared to IDC patients.

Endocrine therapy, also referred to as anti-estrogen therapy, is designed to inhibit ER signaling to slow growth and proliferation of ER+ breast cancer. ER is a nuclear hormone receptor that binds E2 via its ligand binding domain (LBD). Once activated by E2, ER homodimerizes and translocates to the nucleus. This ER homodimer can then bind to an ER-specific estrogen response element (ERE) on DNA to regulate gene transcription and promote cell growth, proliferation, and survival[6]. Frontline treatment for ER+ ILC is frequently anti-estrogen therapy in the form of Aromatase Inhibitors (AI) such as letrozole or Selective Estrogen Receptor Modulators (SERM) such as tamoxifen[7]. AIs act to inhibit aromatase, the enzyme that converts androgen to estrogen (E2), thus restricting E2 biosynthesis and lowering the

concentration of E2 available to activate ER signaling. Conversely, SERMs act directly on ER. SERMs bind the ligand binding pocket of ER to competitively inhibit E2:ER binding and prevent ligand activation of ER. Retrospective analysis shows that compared patients with ER+ IDC vs ER+ ILC found that while ILC patients did show increased benefit from adjuvant letrozole therapy compared to IDC patients, ILC patients that received adjuvant tamoxifen treatment were more likely to have recurrence compared to IDC patients who received the same therapy[8]. This *de novo* resistance to tamoxifen and differential response to endocrine therapy seen in the clinic is also observed in ILC cell lines, but is not currently well understood[2,9]. Further investigation of ILC biology, particularly ER regulation and function, is needed in order to improve treatment options and outcomes for ILC patients.

Studies focused on ILC biology have shown that there are distinct genetic differences in ILC and IDC in mutations of key transcriptional regulatory proteins. GATA Binding Protein 3 (GATA3) is a well-studied transcription factor that cooperates with and regulates ER function[10,11]. Forkhead Box A1 (FOXA1) binds to and opens chromatin prior to ER:DNA binding and is classified as a "pioneer factor[12,13]." Absent FOXA1, ER binding to DNA and subsequent transcription of ER target genes is heavily diminished. ILC has a lower incidence of GATA3 mutations compare to IDC (5% vs 13%), but a higher incidence of mutations in the aforementioned pioneer factor FOXA1 (7% vs 2%)[5]. This is of particular interest because GATA3 and FOXA1 function in concert to regulate ER function, and their mutational differences in ILC and IDC suggest different ER regulation mechanisms in these tumor types. Differences in gene expression profiles and ER target gene regulation have also been reported in ILC vs IDC[14]. A comparison of E2-regulated genes in the IDC cell line MCF7 and the ILC cell

line MM134 identified 85 genes, including *WNT4, PDE4B, and TFCP2L1*, that were E2-regulated and ER-dependent in ILC but not in IDC[15,16].

To understand ER regulation, it is essential to identify and investigate the co-regulator proteins that interact with ER. Co-regulator proteins are proteins that interact with transcription factors to control their transcriptional function[6,17]. These transcriptional modulators are often epigenetic enzymes or scaffolds for epigenetic enzymes, and they work to either promote or repress recruitment of transcriptional machinery to the gene locus. As such, co-regulators are often referred to as "co-activators" or "co-repressors" depending on if they activate or repress transcription[18]. Importantly, co-regulator cohorts and co-regulator expression is often tissue specific, and had been shown to contribute to anti-estrogen resistance in breast cancer[6,19–21]. Elevated expression of Steroid Receptor Coactivator SRC1, an ER co-regulator, in breast cancer tissue is associated with poor response to adjuvant tamoxifen and has shown to also contribute to AI resistance[19]. A recent study reported that FEN1 acts as an ER co-regulator in breast cancer by facilitating formation of a transcriptional complex with ER, and that inhibition of FEN1 block proliferation of tamoxifen resistant breast cancer cells[20]. The tumor suppressor neurofibromin (*NF1*) has also been recently identified as a transcriptional co-repressor of ER, and depletion of NF1 in ER+ breast cancer contributes to AI resistance and tamoxifen agonism[21]. Interplay between ER and its co-regulator cohort drives breast cancer cell proliferation and survival as well as therapy response, and thus represent potential therapeutic targets.

To this end, we performed Rapid Immunoprecipitation Mass Spectrometry of Endogenous Proteins (RIME) to identify novel ER-associated proteins in ILC cells[22,23]. Mediator of DNA Damage Checkpoint 1 (MDC1) was found to be a top hit from this screen. MDC1 is well studied for its role in DNA Damage Response (DDR), where it functions as a scaffold for

other DDR proteins at damaged DNA loci[24–26]. MDC1 has previously been identified as an ER-binding protein and androgen receptor (AR) co-regulator, but has never been studied in the context of ILC[27,28]. The goal of our study is to determine how MDC1 regulates ER function in ILC.

RESULTS

RIME identifies novel ILC-specific ER-associated proteins

We hypothesized that the unique function of ER in ILC is due to ILC-specific ER co-regulator proteins. To identify putative novel co-regulators, we profiled ER-associated proteins in ILC models using the co-immunoprecipitation/mass spectrometry (co-IP/MS) method RIME (Rapid Immunoprecipitation Mass spectrometry of Endogenous proteins). ER-positive ILC cell lines MDA MB 134VI (MM134), SUM44PE (44PE), and BCK4 were grown in full serum and treated with either vehicle (0.1% EtOH) or 1μM 4-hydroxytamoxifen (4OHT). Based on the reduced response on ILC to Tamoxifen in clinical settings, we initially predicted that 4OHT condition would identify ER:protein interactions that mediate partial agonist activity of 4OHT in ILC cells. However, the 4OHT condition result did not reveal any significant changes to the ER interactome. We then combined the vehicle- and 4OHT-treated sample results and identified 416, 231, and 333 ER-interacting proteins in MM134, 44PE, and BCK4, respectively (Figure 1A). For further analysis, we selected ER-associated proteins identified in at least 2 ILC models, which resulted in n=188 proteins. With the aim of identifying ILC-specific ER-interacting proteins, we compared these 118 proteins to published ER RIME data from IDC cells lines MDC7 and ZR75-1 (unions, n=713)[10,22]. This comparison identified n=115 ILC-specific ER-associated proteins and n=73 ER-associated proteins shared in ILC and IDC (Figure 1B).

To begin to understand the functional significance of these ILC-specific ER-associated proteins, the sets were queried in the STRING database to identify functional protein networks (Figure 1C-E)[29,30]. Among ILC-specific ER-associated proteins, we identified a network of epigenomic regulators and co-regulators including DNMT1, BRD4, and KMT2D. ILC-specific ER-associated proteins also show a DNA synthesis and repair network that includes FEN1 and

POLD2 (Figure 1C, E). ER-associated proteins shared in ILC and IDC included a protein regulatory network of well-established ER co-regulators such as EP300, GATA3, FOXA1, and GREB1 (Figure 1D, E). The identification of these ILC-specific ER-associated proteins supports our hypothesis that novel ER:protein interactions may regulate ER function in ILC.

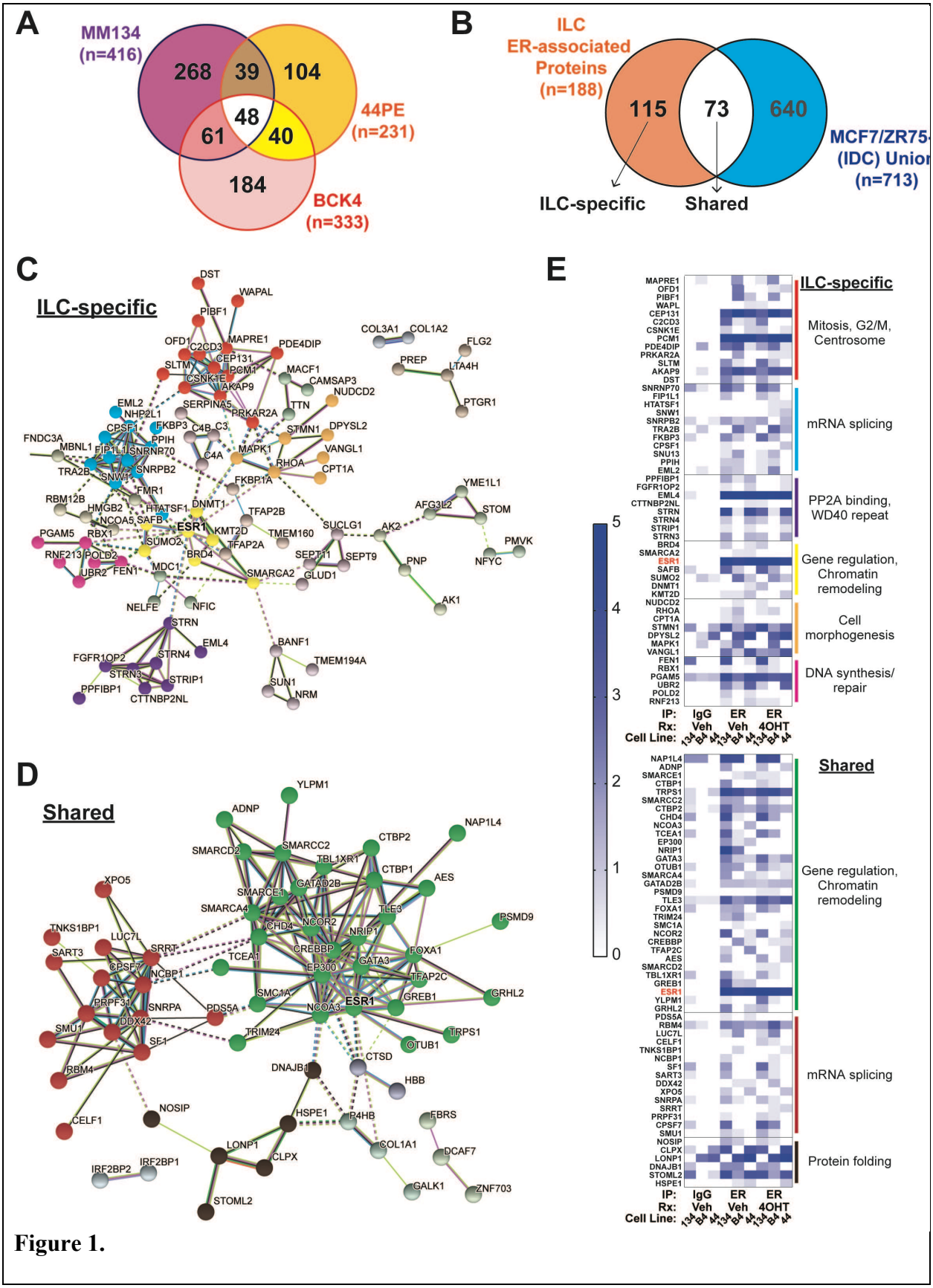
A
MM134
(n=416)
268
39
104
48
61
40
44PE
(n=231)
184
BCK4
(n=333)
B
ILC
ER-associated
Proteins
(n=188)
115
73
640
MCF7/ZR75-
(IDC) Unior
(n=713)
ILC-specific
Shared
C
ILC-specific
DST
WAPAL
PIBF1
OFD1
C2CD3
MAPRE1
PDE4DIP
CEP131
SLTM
PCM1
MACF1
CSNK1E
CAMSAP3
AKAP9
NUDCD2
EML2
NHP2L1
SERPINA5
PRKAR2A
TTN
CPSF1
FKBP3
C4B
C3
STMN1
DPYSL2
FNDC3A
PPIH
MBNL1
FIP1L1
SNRNP70
C4A
MAPK1
VANGL1
TRA2B
SNRPB2
RHOA
CPT1A
SNW1
FKBP1A
FMR1
RBM12B
DNMT1
TFAP2B
HMGB2
HTATSF1
NCOA5
SAFB
ESR1
KMT2D
SUCLG1
PGAM5
RBX1
SUMO2
TMEM160
TFAP2A
RNF213
POLD2
BRD4
SEPT11
SEPT9
MDC1
UBR2
FEN1
SMARCA2
GLUD1
NELFE
NFIC
STRN
EML4
FGFR1OP2
STRN4
STRN3
STRIP1
PPFIBP1
CTTNBP2NL
BANF1
TMEM194A
SUN1
NRM
COL3A1
COL1A2
FLG2
PREP
LTA4H
PTGR1
YME1L1
AFG3L2
STOM
PMVK
NFYC
AK2
PNP
AK1
D
Shared
YLPM1
ADNP
NAP1L4
SMARCD2
SMARCC2
CTBP2
TBL1XR1
CTBP1
AES
XPO5
SMARCE1
GATAD2B
SMARCA4
TLE3
PSMD9
TNKS1BP1
CHD4
NCOR2
NRIP1
LUC7L
SART3
SRRT
CREBBP
FOXA1
TCEA1
GATA3
CPSF7
NCBP1
EP300
TFAP2C
SMC1A
ESR1
GREB1
GRHL2
PRPF31
SNRPA
PDS5A
NCOA3
DDX42
SMU1
TRIM24
TRPS1
SF1
OTUB1
CTSD
RBM4
DNAJB1
HBB
NOSIP
CELF1
HSPE1
P4HB
FBRS
LONP1
COL1A1
DCAF7
CLPX
IRF2BP2
IRF2BP1
GALK1
ZNF703
STOML2
E
ILC-specific
MAPRE1
OFD1
PIBF1
WAPL
CEP131
C2CD3
CSNK1E
PCM1
PDE4DIP
PRKAR2A
SLTM
AKAP9
DST
Mitosis, G2/M, Centrosome
SNRNP70
FIP1L1
HTATSF1
SNW1
SNRPB2
TRA2B
FKBP3
CPSF1
SNU13
PPIH
EML2
mRNA splicing
PPFIBP1
FGFR1OP2
EML4
CTTNBP2NL
STRN
STRN4
STRIP1
STRN3
PP2A binding, WD40 repeat
BRD4
SMARCA2
ESR1
SAFB
SUMO2
DNMT1
KMT2D
Gene regulation, Chromatin remodeling
NUDCD2
RHOA
CPT1A
STMN1
DPYSL2
MAPK1
VANGL1
Cell morphogenesis
FEN1
RBX1
PGAM5
UBR2
POLD2
RNF213
DNA synthesis/ repair
5
4
3
2
1
0
IP: IgG ER ER
Rx: Veh Veh 4OHT
Cell Line: 134 B4 44 134 B4 44 134 B4 44
Shared
NAP1L4
ADNP
SMARCE1
CTBP1
TRPS1
SMARCC2
CTBP2
CHD4
NCOA3
TCEA1
EP300
NRIP1
GATA3
OTUB1
SMARCA4
GATAD2B
PSMD9
TLE3
FOXA1
TRIM24
SMC1A
NCOR2
CREBBP
TFAP2C
AES
SMARCD2
TBL1XR1
GREB1
ESR1
YLPM1
GRHL2
Gene regulation, Chromatin remodeling
PDS5A
RBM4
LUC7L
CELF1
TNKS1BP1
NCBP1
SF1
SART3
DDX42
XPO5
SNRPA
SRRT
PRPF31
CPSF7
SMU1
mRNA splicing
NOSIP
CLPX
LONP1
DNAJB1
STOML2
HSPE1
Protein folding
IP: IgG ER ER
Rx: Veh Veh 4OHT
Cell Line: 134 B4 44 134 B4 44 134 B4 44

Figure 1.

Figure 1. ER RIME Identifies Novel ER-Associated Proteins and Protein Networks in ILC Cell Lines. **(A)** ILC cells were treated with vehicle (0.01% EtOH) or 1μM 4OHT for 24 hours prior to ER RIME (IgG control was performed with vehicle condition only.) MS was performed in technical duplicate for each sample (single biological replicate per condition.) Identified peptides were filtered based on having <20% of peptides for a given protein in IgG samples, and then identified protein being present in <40% of studies in the CRAPome database. Common tubulin and ribosomal protein contaminants were also omitted from further analysis. **(B)** Proteins identified in ≥2 ILC cell lines were compared to the union of all proteins identified in ER RIME of IDC models MCF7 and ZR75-1 from Mohammed, 2013 (IDC data were not filtered by IgG or CRAPome as with IDC data.) **(C)** ILC-specific ER-associated proteins (n=115; plus ER/ESR1, total n=116) were used for network analysis used the STRING database (v11.0, Oct 2019).) Colored clusters were generated in STRING using the MCL clustering option, with inflation parameter = 2. **(D)** STRING network analysis as in (C) for ER-associated proteins common to ILC and IDC (n=73, including ER.) **(E)** Clusters from (C-D) with >5 members are highlighted; colored bars match cluster colors in (C-D) network maps. Heatmaps show the mean spectral counts of technical duplicates for each protein, per cell line and treatment/IP condition. 134 = MDA MB 134VI; B4 = BCK4; 44 = SUM44PE. Functional notation for clusters listed at right are derived from gene ontology analysis using MSIGDB/DAVID. **(F)** MM134 cells were hormone deprived according to protocol then reverse transfected with siRNA against indicated target protein. 24 hours post siRNA transfection, cells were treated with either E2 or 4OHT. 6 days post siRNA knockdown, dsDNA quantification was performed with Hoechst Assay. dsDNA quantification was normalized to Mock siRNA transfection condition.
Data for this figure was collected and analyzed by Dr. Matthew Sikora.

MDC1 is a Novel ER Associated Protein in ILC

To functionally profile our novel ER-associated proteins and identify ER co-regulators, we performed an siRNA screen against ER-driven growth in MM134 ILC cells. We hypothesized that knocking down a protein important for ER regulation would suppress ER-driven cell proliferation. We selected 133 proteins from RIME for screening and supplemented these targets with co-regulators over-expressed in ER+ ILC versus ER+ IDC (n=27) and transcription factors with binding motifs flanking an ER binding site for the ILC-specific ER target gene *WNT4* (n=31)[16]. MM134 cells were hormone deprived, then treated with siRNA targeting the indicated proteins of interest for 48 hours. siRNA against ER (*ESR1*) and known ER pioneer factor FOXA1 acted as positive controls. 24 hours post siRNA transfection, the cells were treated with E2 or 4OHT. Few siRNAs showed differential suppression of E2- versus 4OHT-induced growth, consistent with the lack of 4OHT-specific ER-associated proteins by RIME.

Overall, we identified 82 putative ER co-regulators for which ER-driven proliferation was suppressed by siRNA (Figure 2A). Additionally, because AR can drive growth independently of ER in MM134, we treated cells with synthetic androgen Cl-4AS-1 and assessed cell proliferation by dsDNA quantification six days post-treatment (Figure 2B). Knockdown of MDC1 did not significantly alter Cl-4AS-1 driven growth, indicating that MDC1 is specifically required for ER function and does not regulate AR-driven growth.

Having determined that MDC1 was important for ER-driven proliferation in MM134 cells, we wanted to understand how MDC1 effected proliferation in different ILC cell lines, as well as in IDC cell lines. ILC cells (44PE, CAMA-1) and IDC cells (HCC1428, T47D) were treated with non-targeting siRNA (siNT) or siRNA targeting MDC1 (siMDC1), and growth was

assessed 6 days post transfection (Figure 2B). MDC1 knockdown starkly inhibited growth relative to siNT in both ILC cell lines, but not in the IDC cell lines. Taken together, this data show that MDC1 is specifically required for ER function and supports ER-driven proliferation in ILC cells but not IDC cells.

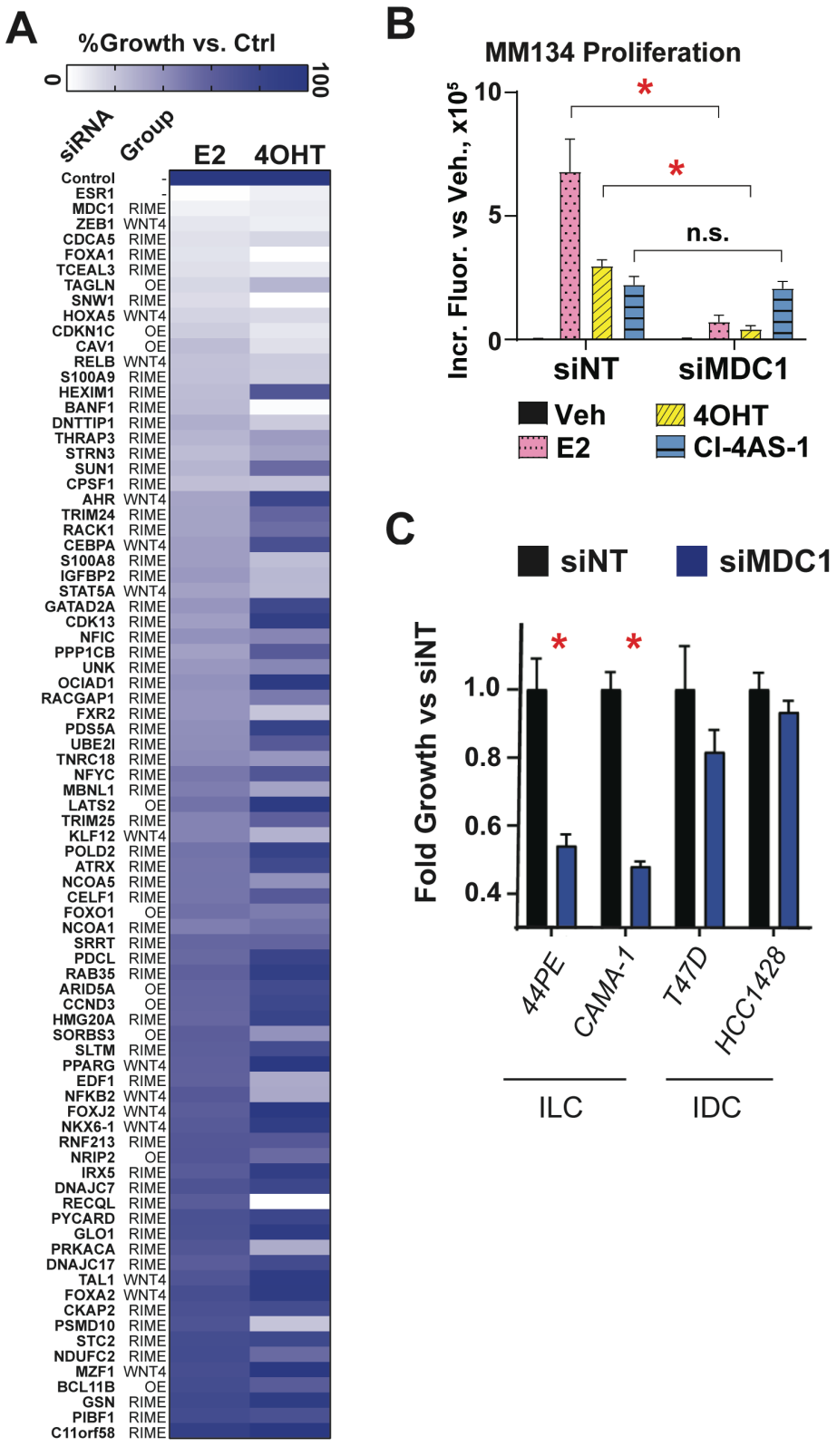
A
%Growth vs. Ctrl
0
100
siRNA
Group
E2
4OHT
Control -
ESR1 -
MDC1 RIME
ZEB1 WNT4
CDCA5 RIME
FOXA1 RIME
TCEAL3 RIME
TAGLN OE
SNW1 RIME
HOXA5 WNT4
CDKN1C OE
CAV1 OE
RELB WNT4
S100A9 RIME
HEXIM1 RIME
BANF1 RIME
DNTTIP1 RIME
THRAP3 RIME
STRN3 RIME
SUN1 RIME
CPSF1 RIME
AHR WNT4
TRIM24 RIME
RACK1 RIME
CEBPA WNT4
S100A8 RIME
IGFBP2 RIME
STAT5A WNT4
GATAD2A RIME
CDK13 RIME
NFIC RIME
PPP1CB RIME
UNK RIME
OCIAD1 RIME
RACGAP1 RIME
FXR2 RIME
PDS5A RIME
UBE2I RIME
TNRC18 RIME
NFYC RIME
MBNL1 RIME
LATS2 OE
TRIM25 RIME
KLF12 WNT4
POLD2 RIME
ATRX RIME
NCOA5 RIME
CELF1 RIME
FOXO1 OE
NCOA1 RIME
SRRT RIME
PDCL RIME
RAB35 RIME
ARID5A OE
CCND3 OE
HMG20A RIME
SORBS3 OE
SLTM RIME
PPARG WNT4
EDF1 RIME
NFKB2 WNT4
FOXJ2 WNT4
NKX6-1 WNT4
RNF213 RIME
NRIP2 OE
IRX5 RIME
DNAJC7 RIME
RECQL RIME
PYCARD RIME
GLO1 RIME
PRKACA RIME
DNAJC17 RIME
TAL1 WNT4
FOXA2 WNT4
CKAP2 RIME
PSMD10 RIME
STC2 RIME
NDUFC2 RIME
MZF1 WNT4
BCL11B OE
GSN RIME
PIBF1 RIME
C11orf58 RIME
B
MM134 Proliferation
Incr. Fluor. vs Veh., x10^5
10
5
0
*
*
n.s.
siNT
siMDC1
Veh
E2
4OHT
CI-4AS-1
C
siNT
siMDC1
Fold Growth vs siNT
1.0
0.8
0.6
0.4
*
*
44PE
CAMA-1
T47D
HCC1428
ILC
IDC

Figure 2.

Figure 2. MDC1 is a Novel Protein Essential for ER-driven growth in ILC
(A-B) MM134 cells were hormone deprived priod to siRNA reverse transfection. 24 hours later, cells were treated with vehicle (0.01% EtOH), 100pM E2, 100nM 4OHT, or 100nM CI-4AS-1 (synthetic androgen). After 6 day, proliferation was measured by dsDNA qauantification via Hoechst Assay. **(A)** Growth vs Mock siRNA control for each treatment condition. "Group" represents context for gene inclusion in siRNA panel. RIME = identified by RIME, WNT4 = transcription factor motif at ER vinding sir in WNT4 gene; OE = over expression in ER+ ILC vs ER+ IDC. **(B)** Data from screen in (A) for siMDC1. *, $p>0.05$; n.s. = not significant; ANOVA w/ Dunnett's multiple correction (analysis from full panel in (A)). **(C)** ILC (44PE, CAMA-1) and IDC (T47D, HCC1428) cells in full serum were reverse transfected with siRNA and growth was assessed 6 days post transfection as previous. *, $p>0.05$, siNT vs siMDC1, Student's T-test.
Data for this figure was collected and analyzed by Dr. Matthew Sikora.

ER:MDC1 Interaction is ILC-Specific

Our ER RIME data indicate that MDC1 is a novel ILC-specific ER-associated protein, and growth data show it may be essential for ER function in ILC. To confirm interaction between ER and MDC1, we performed Proximity Ligation Assays (PLA)[31]. We chose PLA because it allows for *in situ* detection of endogenous protein interactions: Anti-MDC1 and anti-ER primary antibodies of different species bind to endogenous MDC1 and ER, and species-specific secondary antibodies labeled with oligonucleotides bind the primary antibodies. If the secondary antibodies are in close proximity, the addition of DNA polymerase will allow the oligonucleotides ligate and rolling circle amplification will occur, resulting in fluorescent signal (Figure 3A). We performed PLA in a panel of ILC (MM134, 44PE, MM330, CAMA-1) and IDC (MCF7, HCC148, T47D) cell lines. Notably, fluorescent signal indicating ER:MDC1 proximity was observed only in ILC cell lines and not in IDC cell lines (Figure 3B). This is consistent with MDC1 being an ILC-specific ER-interacting protein.

Positive PLA signal indicates proximity of proteins and not necessarily direct binding. To further validate ER:MDC1 interaction, we performed co-immunoprecipitation (Co-IP) assays in the ILC cell lines MM134 and 44PE and IDC cell line MCF7 (Figure 3C). ER:MDC1 interaction was confirmed with ER IP followed by immunoblot of MDC1 in both ILC cell lines, but the interaction was not observed in MCF7 cells. This is consistent with our PLA data and is secondary validation that ER:MDC1 interaction occurs in ILC cells. We were additionally able to confirm MDC1 expression by immunoblot in all ILC and IDC cell lines used for these experiments and validate that siMDC1 does significantly knockdown MDC1 protein levels in all cell lines (Figure 3D). Importantly, Figure 3D also shows that knockdown of MDC1 decreases ER protein levels in both ILC and IDC cell lines. An overall decrease in ER protein levels could

explain the effect of MDC1 knockdown on cell growth in the ILC cells. However, the same growth inhibition is not observed in the IDC cells (Figure 2C) despite the fact that ER protein levels were reduced in response to siMDC1 in both ILC and IDC cells. The effect of MDC1 on ER protein expression will be considered further in the Discussion section.

Using RIME data, we were able to identify possible regions within the MDC1 protein sequence where ER:MDC1 bring may occur. Figure 3E shows a map of the MDC1 protein with known binding motifs labeled (FHA, SDT, TQXF, PST, BRCT)[24]. The orange boxes overlayed over the sequence represent peptide hits from out ER RIME experiments. These are the MDC1 peptides pulled down by ER-IP and identified by our RIME experiment in ILC cells, and as such represent possible regions of the MDC1 protein that facilitate ER:MDC1 binding. Identified with stars are two known nuclear receptor:co-regulator binding motifs, LXXLL (blue) and LXXVL (green)[25]. These motifs are known to confer interaction between nuclear receptors, such as ER, and their co-regulators. Due to the known significance of LXXLL/LXXVL motifs for facilitating ER:co-regulator binding, and the enrichment of peptides in those regions of MDC1 identified by ER RIME, the LXXLL and LXXVL nuclear receptor interaction motifs may be a binding interface for ER:MDC1 in ILC[18].

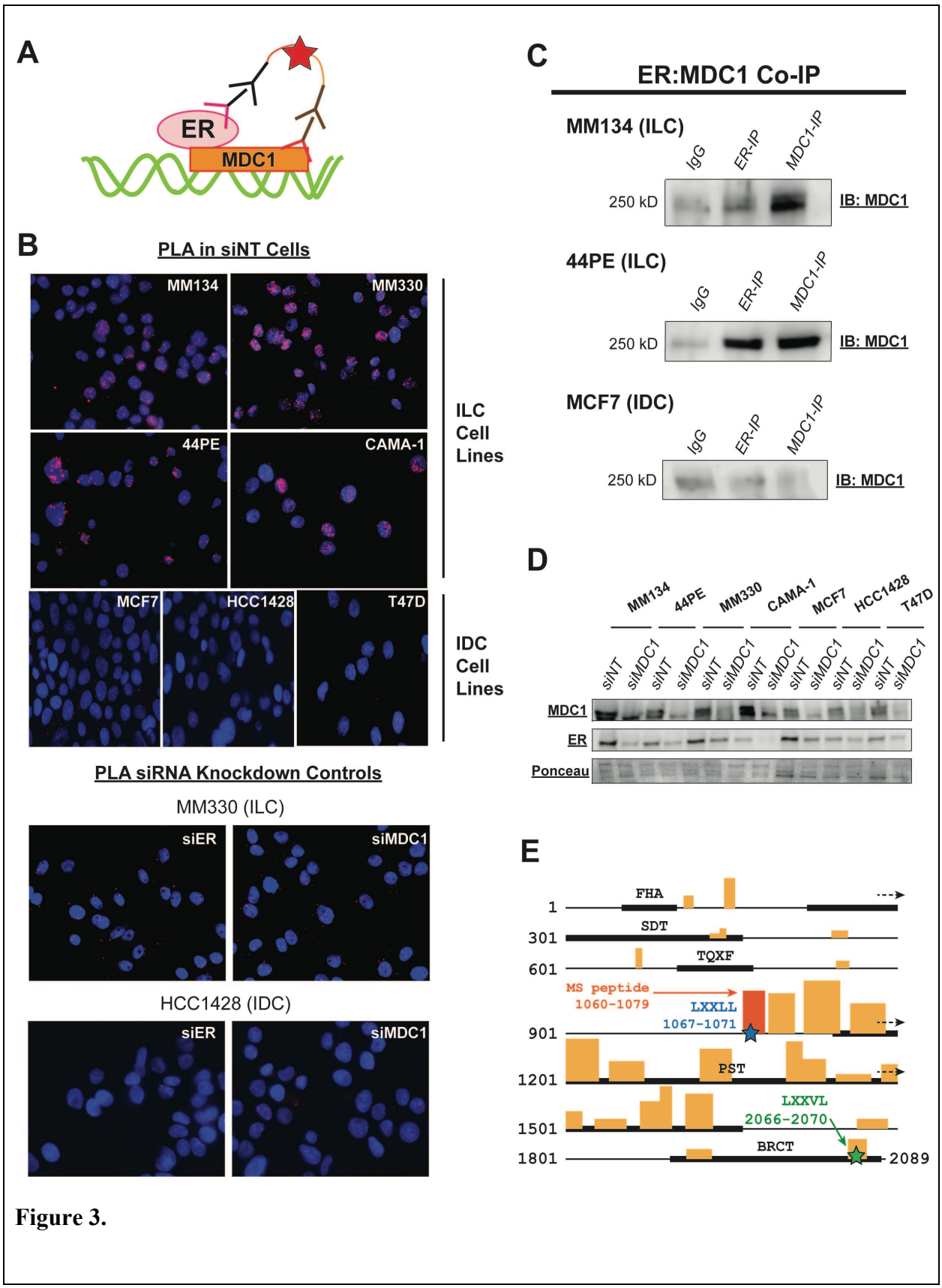
A
ER
MDC1
B
PLA in siNT Cells
MM134
MM330
44PE
CAMA-1
MCF7
HCC1428
T47D
ILC Cell Lines
IDC Cell Lines
PLA siRNA Knockdown Controls
MM330 (ILC)
siER
siMDC1
HCC1428 (IDC)
siER
siMDC1
C
ER:MDC1 Co-IP
MM134 (ILC)
IgG
ER-IP
MDC1-IP
250 kD
IB: MDC1
44PE (ILC)
IgG
ER-IP
MDC1-IP
250 kD
IB: MDC1
MCF7 (IDC)
IgG
ER-IP
MDC1-IP
250 kD
IB: MDC1
D
MM134
44PE
MM330
CAMA-1
MCF7
HCC1428
T47D
siNT
siMDC1
MDC1
ER
Ponceau
E
1
301
601
901
1201
1501
1801
2089
FHA
SDT
TQXF
MS peptide
1060-1079
LXXLL
1067-1071
PST
LXXVL
2066-2070
BRCT

Figure 3.

Figure 3. PLA and Co-IP confirm ER:MDC1 interaction in ILC
(A) Schematic of how PLA experiment identifies protein proximity using primary antibodies of different species against the proteins of interest and species-matched secondary antibodies with conjugated oligonucleotides that bind the primary antibodies. If the secondary antibodies are in close proximity, the addition of DNA polymerase will allow the oligonucleotides ligate and rolling circle amplification will occur, resulting in fluorescent signal that can be identified by immunofluorescence. **(B)** ER:MDC1 PLA results in ILC and IDC cell lines. Red fluorescent signal indicates proximity of ER and MDC1. Cell line in image is indicated in the top right hand corner. Images shown are representative of n=2-6 images for each cell line. siRNA knockdown controls for proteins of interest (ER and MDC1) were performed in both IDC (HCC1428) and ILC (MM330) cells. All images were taken on Zeiss Light Microscope and analyzed with Zeiss microscopy software. **(C)** Reciprocal co-immunoprecitation (co-IP) was performed to confirm ER:MDC1 interaction. ER and MDC1 were pulled down and MDC1 immunoblot was performed to confirm IP and identify protein interactions (antibodies were previously validated). IgG = species matched IgG pull down control. **(D)** ILC and IDC cell lines were reverse transfected with non-targeting (NT) siRNA or siRNA targeting MDC1 (M) for 48 hours prior to lysate harvest for immunoblot. Control condition (no siRNA transfected) is shown in "-" lanes. **(E)** Diagram of MDC1 protein with known binding regions labeled (FHA, SDT, TQXF, PST, BRCT) and indicated with thick black lines. Orange boxes represent MDC1 peptide hits identified by ER RIME. The blue star indicates the location of the LXXLL nuclear receptor binding motif, and the green star represents the location of the LXXVL motif in the MDC1 protein. *Co-IP data in this figure was collected by Dr. Joseph Sottnik.*

MDC1 Regulates ER Transcriptome in ILC

After confirming ER:MDC1 interaction in ILC, we sought to understand the functional implications of this novel interaction. We hypothesized that because knockdown of MDC1 resulted in a stark ablation of E2-driven growth in ILC (Figure 2D), MDC1 may be similarly required for ER gene regulation. Of note, though MDC1 is primarily involved in DNA damage response (DDR), studies have implicated MDC1 as a putative interacting protein with both ER and AR[27,28]. We tested the effect of siMDC1 on E2-induced ER target gene expression in ILC (MM134) and IDC (HCC1428) cells by qPCR. MDC1 knockdown ablated regulation of many ER target genes in ILC cells. Induction of *WNT4, IGFBP4, PDZK1, and TFCP2L1*, and repression of *PDE4B* were blocked (Figure 4A). However, ablation of ER target gene regulation by siMDC1 was not universal as *TFF1* induction in MM134 was unaffected, and no effect was observed in HCC1428. Expression of *ESR1* was downregulated in response to MDC1 knockdown in both the ILC and IDC cell lines, which corroborates immunoblot data in Figure 3D showing that siMDC1 decreases ER protein levels in ILC and IDC cells.

To identify the component of the ER transcriptome that requires MDC1 in ILC cells, we performed RNA-sequencing (RNAseq) following MDC1 knockdown in ILC models MM134 and MM330, and IDC model HCC1428 (Figure 4B). *ESR1* knockdown (siESR1) was included as a positive control and filter for ER target genes. *FOXA1* knockdown (siFOXA1) was also included because the effect of FOXA1 on ER-driven transcription is well studied[13]. FOXA1 is a pioneer factor that facilitates ER binding to chromatin, and we wanted to compare the effect MDC1 knockdown to knockdown of a well-studied ER-associated protein to provide context for the role of MDC1 on the ER transcriptome.

This approach determined that MDC1 is required for a large proportion of the ER-driven transcriptome, and identified gene sets within the ER transcriptome that were regulated by either MDC1 (MDC1 only, pink) or FOXA1 (FOXA1 only, green), both factors (MDC1+FOXA1, orange), or neither factor (ER only, black) (Figure 4C). A guide to the different gene regulation sets and their color-coding is shown in Figure 4D. In MM134 cells, among n=3599 ER target genes, 57.3% were dysregulated upon MDC1 knockdown, and a similar proportion were dysregulated by FOXA1 knockdown (56.1%). This included genes dysregulated by either MDC1 or FOXA1 knockdown (n=1387, 38.5%), but 18.8% (n=675) and 17.6% (n=633) of ER target genes required specifically MDC1 or FOXA1, respectively. As expected, FOXA1 knockdown also dysregulated a majority of ER target genes in MM330 and HCC1428 (54.0% and 59.9%, respectively), while MDC1 played a smaller role in the ER transcriptome in these cells compared to MM134 (23.9% and 32.1% of ER target genes in MM330 and HCC1428, respectively).

Since siMDC1 dysregulated a large proportion of the ER transcriptome in both ILC and IDC cells, despite protein interaction assays showing ER:MDC1 interaction to be ILC-specific, we examined regulatory pathways differentially effected by MDC1 knockdown in each cell line. When using the entire geneset dysregulated by siMDC1 (including MDC1+FOXA1 co-targets), the MsigDB Hallmark signatures for estrogen response were enriched in all 3 models, along with mTORC1 signaling, a known downstream component of ER signaling. However, we noted that the Hallmark DNA repair pathway was enriched specifically in HCC1428; this was similarly observed when enrichment was performed against Reactome genesets (Figure 4E). Differential enrichment of DNA repair pathways in the ILC v IDC models suggests the effect of siMDC1 on ER-driven transcription in IDC is similar to canonical MDC1 function in a DDR, but not in ILC cells where MDC1 is acting as an ER co-regulator.

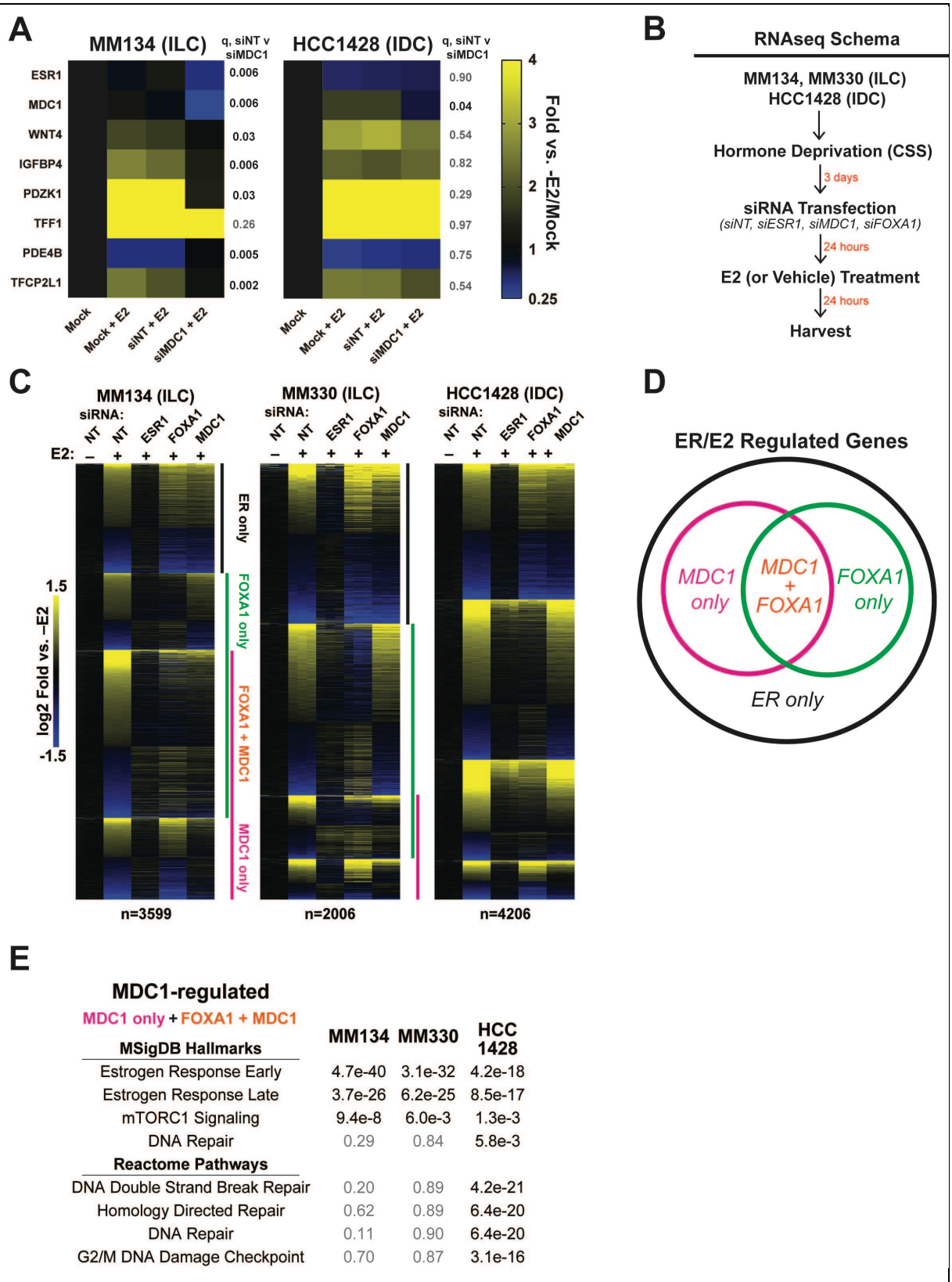

MDC1-regulated

MDC1 only + FOXA1 + MDC1

MSigDB Hallmarks	MM134	MM330	HCC 1428
Estrogen Response Early	4.7e-40	3.1e-32	4.2e-18
Estrogen Response Late	3.7e-26	6.2e-25	8.5e-17
mTORC1 Signaling	9.4e-8	6.0e-3	1.3e-3
DNA Repair	0.29	0.84	5.8e-3
Reactome Pathways			
DNA Double Strand Break Repair	0.20	0.89	4.2e-21
Homology Directed Repair	0.62	0.89	6.4e-20
DNA Repair	0.11	0.90	6.4e-20
G2/M DNA Damage Checkpoint	0.70	0.87	3.1e-16

Figure 4.

Figure 4. MDC1 Differentially Regulates ER Transcriptome in ILC vs IDC
(A) MM134 and HCC1428 cells were hormone deprived according to protocol (see Materials and Methods), then plated and transfected with non-targeting siRNA (siNT) siRNA against MDC1 (siMDC1). Mock condition with no siRNA transfection is also included. 24 hours post transfection, vehicle or 1nM E2 was added. 48 hours post transfections, plate was washed with PBS and frozen at -80ºC. RNA was harvested using illustra RNAspin Mini Kit, and cDNA was synthesized using Promega GoScript Reverse Transcriptase kit. RT-qPCR was performed using QuantStudio 6 Real Time qPCR System. **(B)** Schematic describing how samples were prepared for RNA-seq analysis. **(C)** Hormone deprived MM134, MM330, and HCC1428 cells were transfected with indicated siRNA 24 hours prior to treatment with vehicle (0.01% EtOH) or 1nM E2. ER regulated genes were identified by ligand regulation (siNT vs siNT+E2; $q<0.0001$) and reverse of regulation by siESR1 (siNT+E2 vs siESR1+E2, $q<0.0001$). For MM330, a less stringent ligand regulation cutoff was used ($q<0.01$) due to known ligand-independent activity of ER in this cell line. **(D)** Schematic representing the different gene regulation groups identified and described herein. All gene sets are identified within the set of ER/E2 regulated genes (black circle). MDC1 only (pink) genes and FOXA1 only (orange) genes were identified within this larger ER/E2 regulated gene set, and their overlap represent genes regulated by both MDC1 and FOXA1 (orange). Genes regulated by neither FOXA1 or MDC1 are indicated as having "ER only" regulation. **(E)** MDC1 regulated ER target genes (pink circle excluding overlap in Fig 3D) were subject to over-representation analysis (ORA) against MSigDB genesets (Top: H, C2/CP, C6; Bottom: C2/Reactome).
RNA-seq data analysis was performed by Dr. Matthew Sikora and the University of Colorado Anschutz Medical Campus Bioinformatics Core.

DISCUSSION

Project Summary and Conclusions

ILC represents an understudied breast cancer histotype that is typically diagnosed at a later stage and studies in ILC cell lines show *de novo* resistance to Tamoxifen treatment[2,9]. Differential response to ER-targeted therapy indicates ILC-specific ER regulation and function. ER-driven cancer cell proliferation and survival has been shown to be critically dependent on tissue-specific co-regulator cohorts. Approximately 95% of ILC cases express ER, and as such identifying and investigating ER co-regulators in ILC is essential for understanding ILC biology and developing ILC-specific therapies. Defining ILC-specific ER co-regulators is also important for understanding this resistance and developing ILC-specific treatment options. We performed an unbiased analysis of ER RIME results and identified MDC1 as a putative novel ER associated in ILC.

MDC1 canonically functions as a scaffolding protein in repair of DNA double stranded breaks (DSBs). Importantly, MDC1 does not have any intrinsic enzymatic function but instead scaffolds DDR proteins with enzymatic function. Upon induction of DSBs, the histone variant H2AX is incorporated at the site of the break and phosphorylated at the C-terminal serine residue by phosphatidylinositol 3-kinase-related kinases (PIKKs)[24]. The phosphorylated form is H2AX is termed γH2AX and serves as an epigenetic marker of DSBs. The C-terminal BRCT domain of MDC1 binds γH2AX and mediates interactions between the damaged DNA and essential DNA repair proteins[26]. These DDR proteins include the MRN complex, which binds the SDT domain of MDC1, and the E3 ubiquitin ligase RNF1, which binds to the TQXF domain. To facilitate these and other protein interactions, MDC1 is heavily post translationally modified[33]. Absence of

MDC1 severely diminishes repair of damaged dsDNA, and as such is it considered an essential adaptor protein in DDR.

Our study suggests a novel role for MDC1. Data show MDC1 is integral for ER-driven growth in multiple ILC cell lines and is separate from AR-driven growth processes. Conversely, MDC1 did not inhibit growth in our IDC cell lines. Protein interaction assays confirm that MDC1 interacts with ER uniquely in ILC: PLA data show ER:MDC1 association in all 4 ILC cell lines, but not in our 3 IDC cell lines. Co-IP results have validated this interaction in both our MM134 and 44PE ILC cell lines. Having confirmed that MDC1 is an ILC-specific ER-interacting protein, we sought to understand the functional significance of this novel interaction. We investigated the effect of MDC1 knockdown on E2-driven ER target gene expression in both ILC (MM134) and IDC (HCC1428) cells. We found that MDC1 ablates regulation of ER target genes in ILC cells, but that this ablation is not universal to all ER target genes. Consistent with our findings from PLA and co-IP, MDC1 knockdown does not affect ER target gene transcription in the IDC cell line.

Immunoblot and qPCR data show that knockdown of MDC1 lowers ER expression at both the mRNA and protein level in ILC and IDC. An overall reduction in ER levels could explain why MDC1 effects cell proliferation, ER target gene transcription, and ER:DNA binding. However, we observed these effects only in ILC and MDC1 knockdown decreases ER levels in both ILC and IDC. Previous studies have shown that FOXA1 knockdown also decreases ER expression in breast tissue[34]. This effect is in addition to the established role of FOXA1 as an ER pioneer factor, thus it is likely that MDC1 can influence ER expression in addition to acting as an ER transcriptional co-regulator in ILC. While our RNA-seq data show that a large subset of ER/E2 regulated genes are dependent on MDC1 in both ILC and IDC,

pathway analysis shows that MDC1 is regulating distinct functions in ILC vs IDC. In ILC, MDC1 regulates genes related to E2-response, whereas in IDC, MDC1 regulates genes related to DNA repair and the G2/M DNA Damage Checkpoint. So while MDC1 knockdown does decrease ER levels in ILC and IDC, this decreased expression does not explain the differential role of MDC1 in ILC and IDC. Further investigation into the role of MDC1 in ILC vs IDC is necessary for the future of this project. Taken together, the data presented herein indicate that MDC1 is a novel ILC-specific ER-interacting protein that regulates ER-driven transcription to promote ILC proliferation.

Future Directions Based on Preliminary Data

Identifying MDC1 as a novel ER-coregulator in ILC is an exciting development in the understanding of ILC biology. However the mechanism by which MDC1 regulates ER-driven transcription is yet to be discerned, and this is crucial if we are to inhibit MDC1-controlled ER function therapeutically. To this end, we have begun investigating how MDC1 may regulate ER binding to DNA at ER-target gene loci. Using two different anti-MDC1 antibodies, we performed ChIP and used qPCR to determine if both ER and MDC1 are binding at two known ER binding sites (ERBS) in ILC (*WNT4* and *IGFBP4*). We confirmed ER binding at both loci and demonstrated MDC1 co-binding using two different anti-MDC1 antibodies (Figure 5A).

Our preliminary data futher show that MDC1 may be binding DNA at ER-target gene loci in ILC. Future work on this project will need to include further MDC1 ChIP-qPCR experiments to validate MDC1:DNA binding at *WNT4* and *IGFBP4* loci, as well as other ER-target gene loci in ILC including loci of genes identified to be MDC1-dependent by our RNA-seq analysis. In addition to assessing ER:DNA binding, we wanted to investigate if MDC1 regulates ER binding to DNA at ER-target gene loci. We again performed ER ChIP-qPCR, and

evaluated how knockdown of MDC1 or FOXA1 effected ER:DNA binding at four ER target gene loci (*WNT4, TFCP2L1, PDE4B, TFF1*). Importantly, our qPCR analysis shows that E2-driven transcription of *WNT4, TFCP2L1,* and *PDE4B* are MDC1 regulated, while *TFF1* is not dependent on MDC1. Knockdown of pioneer factor FOXA1 diminishes ER:DNA binding at all four loci (Figure 5B). Consistent with our qPCR data, MDC1 knockdown inhibits ER:DNA binding at *WNT4, TFCP2L1,* and *PDE4B* ERBS but not at the *TFF1* ERBS. We were additionally able to demonstrate that FOXA1 and MDC1 knockdown also decrease ER binding at the *IGFBP4* ERBS (Figure 5C). However, our data suggest that MDC1 knockdown may also decrease FOXA1:DNA binding at this locus. This is especially interesting as the function of FOXA1 as an ER pioneer factor is well-studied and established, and novel regulation of FOXA1 by MDC1 could have extensive implications for distinctive ER regulation in ILC.

To further discern how MDC1 effect FOXA1, we first looked at the effect of MDC1 knockdown on FOXA1 protein by immunoblot and found that absence of MDC1 does not significantly affect FOXA1 protein levels (Figure 5D). We then performed Dual PLA to assess binding of ER:MDC1 and ER:FOXA1 in our MM134 ILC cells[35]. Dual PLA allows for fluorescent detection two endogenous protein:protein interactions simultaneously (Figure 5E). In this assay, both interactions are detected separately, and detection of one binding interaction is not dependent on the other. We found that in the non-targeting siRNA (siNT) cells, ER interacts with both FOXA1 (ER:FOXA1, yellow) and MDC1 (ER:MDC1, purple, Figure 5F). As expected, the ER knockdown cells show diminished PLA signal for both ER:FOXA1 and ER:MDC1. Interestingly, knockdown of FOXA1 or MDC1 similarly decreased PLA foci for both interactions. PLA foci for each interaction are detected independently in dual PLA, so this suggests a possible interdependence between ER, FOXA1, and MDC1 binding. Results from our

future ChIP-qPCR experiments investigating the effect of MDC1 on FOXA1:DNA binding will help develop our understanding of how these proteins act in consort and control their binding interactions.

We have shown ER:MDC1 binding in ILC cells in E2-replete conditions and demonstrated that MDC1 regulates E2-driven ER-target gene transcription in ILC. We then asked if the ER:MDC1 interaction was ligand dependent (i.e. if is E2 required for ER:MDC1 binding). To this end, we performed co-IP in MM134 cells with the following conditions: Replete cells (Replete), hormone deprived cells with E2 added back (+E2), and hormone deprived cells without E2 (-E2, Figure 5F). ER:MDC1 binding was found to occur in all conditions, indicating that the ER:MDC1interaction is not E2-dependent. This preliminary finding was unexpected because canonically, ER binds E2 to then translocate to the nucleus and bind DNA. If the ER:MDC1 interaction is in fact ligand independent, this indicates that the ER:MDC1 interaction may occur independent of ER:DNA binding. To fully understand the mechanism of MDC1 as a novel ER co-regulator in ILC, future work on this project must determine where in the cell ER:MDC1 binding occurs.

We have shown that MDC1 is a novel ER interacting protein, and that this interaction occurs specifically in ILC cell lines. Our data also demonstrate MDC1 regulates significant portions of the ER transcriptome. Preliminary data indicate that MDC1 may control ER binding to DNA at ER target gene loc and may also influence ER:FOXA1 binding. We have additionally shown that interaction between ER and MDC1 may be E2-independent, and as such ER:MDC1 binding may not arise on DNA. Taken together, these data demonstrate that MDC1 is a novel ILC-specific ER coregulator that controls ER-driven transcription and lay a strong foundation for establishing the mechanism by which MDC1 regulates ER functions. The following model is

proposed based on this data for how MDC1 acts as an ER co-regulator in ILC (Figure 6). We posit that ER, FOXA1, and MDC1 exist in complex. Similar to its role in DDR, MDC1 acts as a scaffolding protein that binds other co-regulators with enzymatic function to this complex. This large complex then acts to recruit DNA Polymerase II to the gene locus to promote ER target gene transcription.

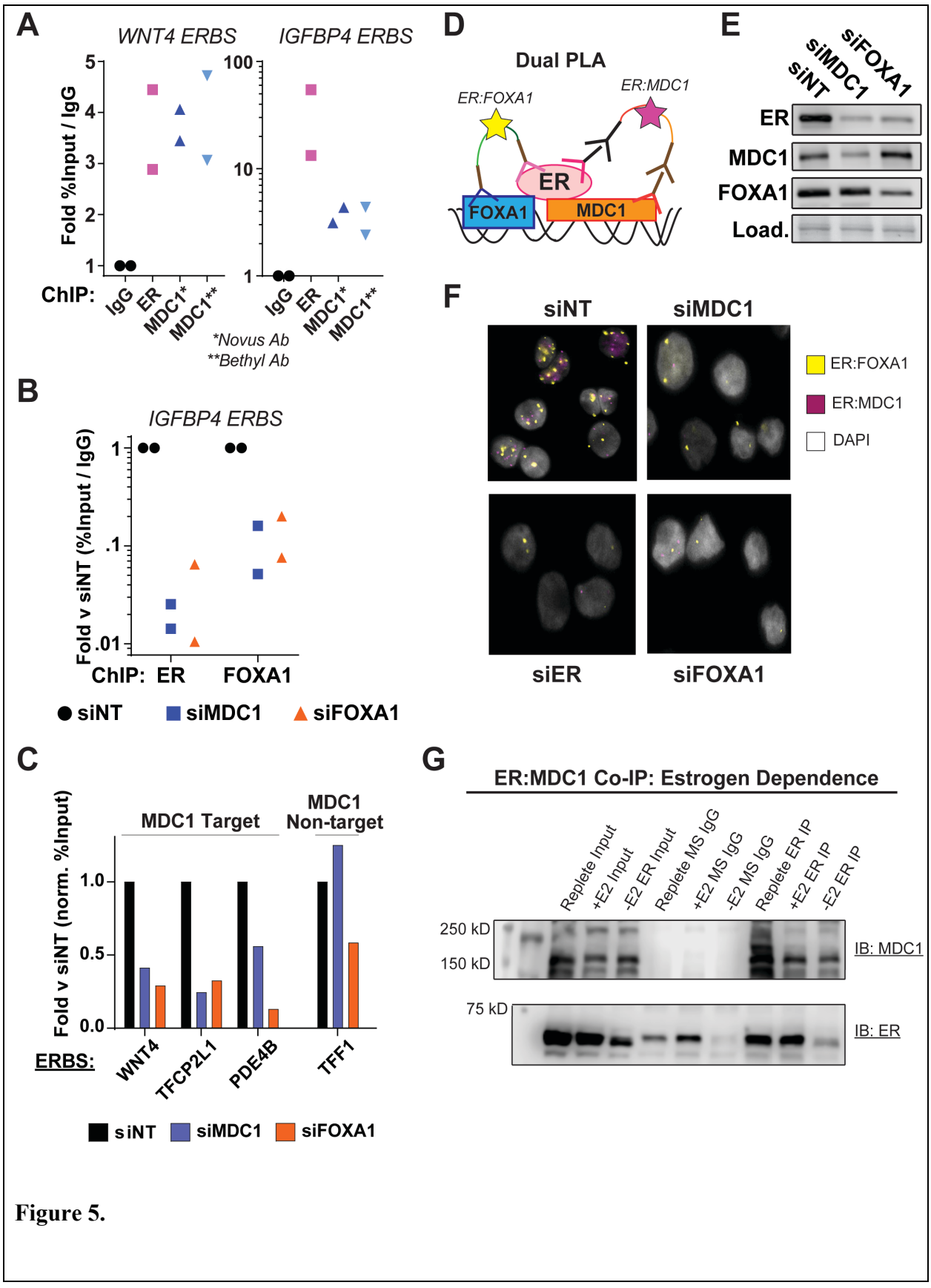
A
WNT4 ERBS
IGFBP4 ERBS
Fold %Input / IgG
ChIP:
IgG
ER
MDC1*
MDC1**
*Novus Ab
**Bethyl Ab
B
IGFBP4 ERBS
Fold v siNT (%Input / IgG)
ChIP: ER
FOXA1
siNT
siMDC1
siFOXA1
C
MDC1 Target
MDC1 Non-target
Fold v siNT (norm. %Input)
ERBS:
WNT4
TFCP2L1
PDE4B
TFF1
siNT
siMDC1
siFOXA1
D
Dual PLA
ER:FOXA1
ER:MDC1
ER
FOXA1
MDC1
E
siNT
siMDC1
siFOXA1
ER
MDC1
FOXA1
Load.
F
siNT
siMDC1
ER:FOXA1
ER:MDC1
DAPI
siER
siFOXA1
G
ER:MDC1 Co-IP: Estrogen Dependence
Replete Input
+E2 Input
-E2 ER Input
Replete MS IgG
+E2 MS IgG
-E2 MS IgG
Replete ER IP
+E2 ER IP
-E2 ER IP
250 kD
150 kD
IB: MDC1
75 kD
IB: ER

Figure 5.

Figure 5. Preliminary Data for Understanding the Mechanism of MDC1 as an ER Co-Regulator
(A) ChIP-qPCR for ER and MDC1 binding at the IGFBP4 and ENT4 ER binding sites (ERBS). MDC1 ChIP was performed with two independent anti-MDC1 antibodies (*Novus Biologics anti-MDC1 antibody, ** Bethyl Laboratories anti-MDC1 antibody). Species matched IgG control was included and used for normalization (Fold %Input/IgG). **(B)** ER ChIP-qPCR for binding at the WNT4, TFCP2L1, PDE4B, and TFF1 ERBS in response to MDC1 and FOXA1 siRNA knockdown. "MDC1 Target" or "MDC1 Non-Target" is indicated as determined by RT-qPCR results shown above. siNT was used for normalization of qPCR signals. **(C)** ChIP-qPCR for ER and FOXA1 binding at the IGFBP4 locus in response to siRNA knockdown of FOXA1 or MDC1. ChIP target is indicated on the x-axis. Non-targeting siRNA (siNT) was used for normalization of qPCR signals. **(D)** Immunoblot (IB) for ER, MDC1, and FOXA1 in MM134 cells with siRNA against MDC1 and FOXA1 with siNT control. Amido Black was used for the loading control. **(E)** Diagram describing the mechanism of the Dual PLA experiment performed in (F). ER:MDC1 interaction is detected as described in Single PLA. ER:FOXA1 proximity was detected using primary-conjugated antibodies (i.e. the primary antibodies detecting ER or FOXA1 are directly conjugated to the fluorescent oligonucleotide). **(F)** Dual PLA images in MM134 cells with siNT control and siRNA knockdown of ER, MDC1, or FOXA1. ER:FOXA1 proximity is indicated by yellow foci and ER:MDC1 by purple foci. DAPI staining is pseudo-colored as white. **(G)** ER-IP in MM134 replete media cells, hormone deprived cells with E2 re-added, or hormone deprived cells without addition of E2. Species matched (MS = mouse) IgG control included. IB for MDC1 was performed to confirm binding in each condition and ER IB to confirm successful ER-IP.

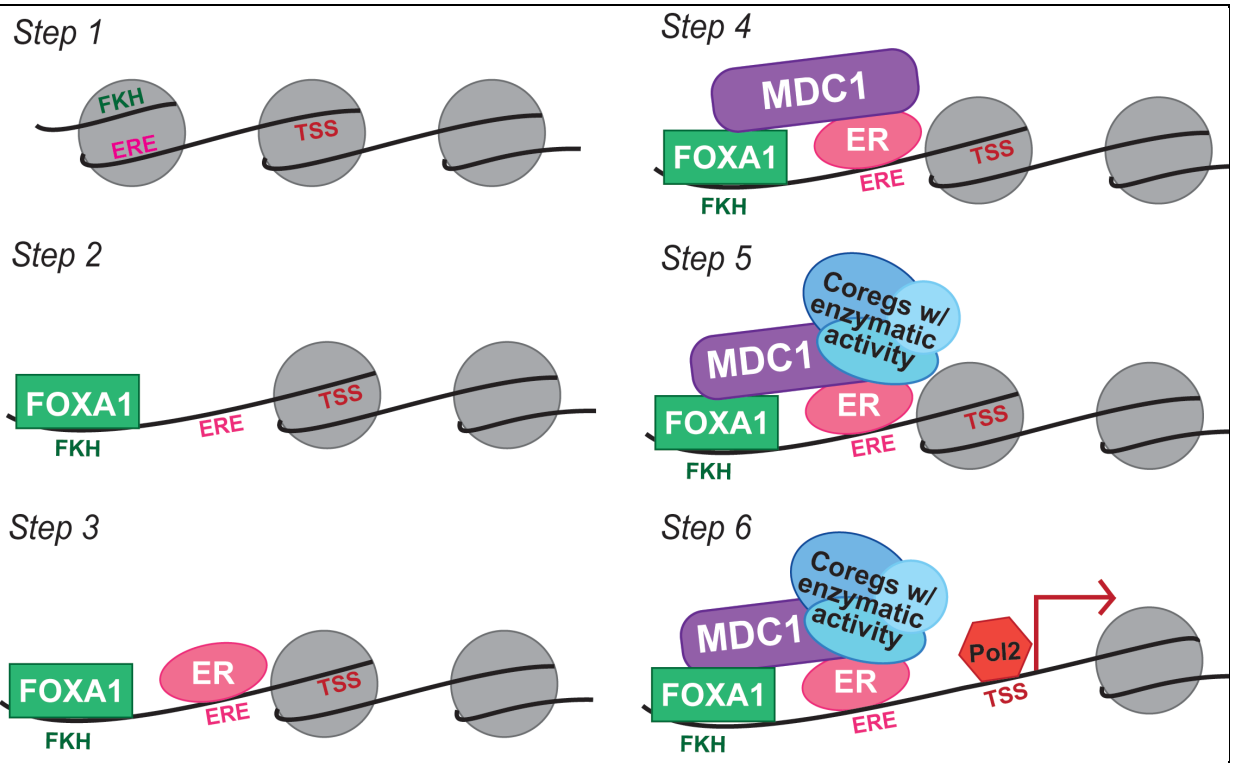

Figure 6

Figure 6. Proposed Model for MDC1 as an ER Co-Regulator in ILC
ER (pink), FOXA1 (green), and MDC1 (Purple) exist in complex. FOXA1 binds the forkhead (FKH) domain and opens chromatin to expose the estrogen response element (ERE). ER then binds the ERE, and MDC1 binds FOXA1 and ER. Similar to its role in DDR, MDC1 then acts as a scaffolding protein that binds other co-regulators (blues) with enzymatic function to this complex. This large complex then acts to regulate ER target gene transcription by recruiting RNA polymerase 2 (red) to the transcription start site (TSS).

MATERIALS AND METHODS

Cell culture and reagents

MDA MB 134VI (MM134; ATCC, Manassas, VA, USA) and SUM44PE (BioIVT, Westbury, NY, USA) were maintained in as described[15]. MDA MB 330 (MM330; ATCC) and HCC1428 (ATCC) were maintained in DMEM/F12 + 10% FBS. MCF7 and CAMA-1 lines were generous gifts from the Rae Lab at the University of Michigan, and were maintained in DMEM/F12 + 10% FBS. T47D were a generous gift from the Sartorious Lab at the University of Colorado, and were maintained in MEM + 5% FBS + 1x Non-essential amino acids + 1nM sodium pyruvate + 1nM insulin. All lines were incubated at 37°C in 5% CO_2. All cell lines were regularly confirmed to be mycoplasma negative and were authenticated University of Colorado Anschutz Tissue Culture Core. Estradiol (E2) and 4-hydroxytamoxifen (4OHT) were obtained from Sigma; ICI 182780 (ICI; fulvestrant) was obtained from Tocris Biosciences. E2, 4OHT, and ICI were dissolved in ethanol, and vehicle treatments are using 0.1% EtOH.

Hormone Deprivation

Cells were seeded at optimum density per cell line in replete media in T75 a flask, and hormone deprivation process begins after the cells are sufficiently adhered. Day 1: Replete media is removed, and cells and entire flask are washed 2x in ~12mL IMEM. IMEM is removed and ~10mL IMEM + 10% charcoal stripped serum (CSS) is added for all cell line excepting SUM44PE, which requires IMEM + 5% CSS. CSS is prepared as previously published and stored at -20ºC[36]. Repeat this 2x wash and media addition at least an hour after the first wash, keeping cells in the incubator during this time. Day 2: Repeat all steps of Day 1, including the break between washing steps. Day 3: Wash cells and flask in IMEM 2x then add 10mL

IMEM+CSS. The proceed to experimental plating, using phenol-red free trypsin and IMEM+CSS for cell media.

siRNA Knockdown

siRNA constructs were reverse transfected using RNAiMAX (ThermoFisher) according to manufacturer instructions. Constructs are siGENOME SMARTpool siRNAs (GE Healthcare Dharmacon, Lafayette, CO, USA) containing 4x siRNA targeting constructs, or individual siRNA constructs: Non-targeting pool #2 (D-001206-14-05), Human *ESR1* pool (M-003401-04-0010), Human *MDC1* pool (M-003506-04-0005), Human *FOXA1* pool (M-010319-01-0005), and Human *MDC1* individual constructs (D-003506-02-0002, D-003506-03-0002, D-003506-05-0002, D-003506-06-0002).

Rapid Immunoprecipitation Mass Spectrometry of Endogenous Proteins (RIME)

RIME was performed with Active Motif (Carlsbad, CA), and samples were prepared according to the provided protocol (https://www.activemotif.com/documents/2053.pdf) and as previously published[22]. Briefly, MM134, 44PE, or BCK4 cells were plated in standard conditions containing FBS (above) in three 15cm plates; 1 plate each was used for Vehicle treatment (ER IP), 4OHT treatment (ER IP), or Vehicle treatment for IgG IP control. Cells were treated with Vehicle (0.1% EtOH) or 4OHT (1μM) for 24hr prior to harvest. At the time of harvest, cells (MM134: ~$9x10^7$/plate; 44PE: ~$3x10^7$/plate; BCK4: ~$2.5x10^7$/plate) were fixed in 11% formaldehyde solution for 8min at room temperature with gentle rocking. Fixation was quenched with 1/20 volume of 2.5M glycine, and cells were collected by scraping. After centrifugation, pellets were washed twice in 0.5% Igepal CA-630 + 1mM PMSF in PBS, then pelleted and snap frozen. Nuclear isolation, immunoprecipitation, and mass spectrometry (in technical duplicates)

were performed by Active Motif. ER IP used antibody sc-543 (Santa Cruz Biotechnology; Santa Cruz, CA; antibody is discontinued).

siRNA Screen

siRNA SMARTpools containing 4 siRNA constructs per pool were ordered as a pre-plated custom libraries in 96-well format (Dharmacon / Horizon Discovery; Layfayette, CO). MM134 cells were hormone-deprived in IMEM + 10% CSS prior to reverse transfection with 10nM siRNA (using RNAiMAX; Thermo Fisher). 24hr post-transfection, cells were treated with Vehicle (0.01% EtOH), 100pM E2, 100nM 4OHT, or 10nM Cl-4AS-1 and allowed to grow for 6 days prior to assessing proliferation by dsDNA quantification (see below).

Immunoblotting

Cells were seeded in 12- or 24-well plates for ~80% confluence according to cell size (MM134 and SUM44PE: 800k/well or 400k/well; MM330: 640k/well or 320k/well; CAMA-1: 400k/well or 200k/well; MCF7 and T47D: 320k/well or 160k/well; HCC1428: 240k/well or 120k/well) and treated with appropriate drug or siRNA concentration. Cell lysates were harvested after treatments in RPPA buffer (50mM HEPES pH 7.4, 150mM NaCl, 1.5mM $MgCl_2$, 1mM EGTA, 10% Glycerol. 1% Triton X-100, dH_2O) with phosphatase inhibitors (ThermoFisher #78420). Membranes were blocked in either 5% milk or 5% BSA in Tris-buffered saline with 0.5% Tween 20, depending on primary antibody used. Primary antibody probing was performed according to manufacturer recommended concentrations, and species-matched secondary antibodies were diluted in matching 5% milk or 5% BSA. Membranes were imaged on LiCor C-DiGit blot scanner.

Co-Immunoprecipitation (Co-IP)

Prior to IP, nuclear extraction was preformed: Cells were rinsed with HBSS+1mM EDTA and collected into tube via scraping. Cells were centrifuged for 5 min at 1000xg and packed cell volume (PCV) was measured. Cells were then resuspended in 5x PCV of PBS, centrifuged for 3 min at 1000xg, then supernatant was aspirated. Pellet was resuspended in 3x PCV of Buffer A (10mM HEPES-KOH, 1.5mM $MgCl_2$, 10mM KCl, 1mM DTT, 1x protease inhibitors) and left on ice for 3 min to swell. Cells were then placed in Dounce homogenizer and "dounced" 10x while on ice, then transferred to tube. The cell suspension was centrifuged at 4ºC for 15 min at 18,000xg, then supernatant was removed and saved as the cytoplasmic fraction. The pellet is the nuclei, and packed nuclear volume (PNV) was measured. Nuclei pellet was resuspended in 2x PNV of Buffer B (20mM HEPES-KOH, 25% Glycerol, 1.5mM $MgCl_2$, 0.6M KCl, 0.2mM EDTA, 1mM DTT, 1x protease inhibitors), and placed in 4ºC cold room on rocker for 45 min. The solution was then pelleted by centrifugation at 4ºC for 10min at 18,000xg. Supernatant was removed and saved, and pellet was resuspended in 3x PNV of Buffer C (20mM HEPES-KOH, 1.5mM $MgCl_2$, 0.2mM EDTA, 0.67% NP40, 1mM DTT, 1x protease inhibitors). Solution was centrifuged at 4ºC for 5 min at 18,000xg to pellet insoluble proteins. ~30uL of nuclear extract was saved as Input control sample, the rest was aliquoted and used for IP.

Nuclear extract supernatant was incubated with appropriate antibody overnight at 4ºC with gentle agitation (ex. rotor). Species matched IgG control IP was performed in tandem. The next day, beads (25uL beads/10ug antibody per sample) were prepared by washing 2x in IP Buffer. Beads were added to each sample and Buffer D was added for a total volume of 500uL per sample. Samples were incubated at 4ºC for 2-4 hours with gentle agitation. Beads were pelleted according to manufacturer recommendations and washed 5x with 1mL of Buffer D.

Protein complexes were eluted by adding 100uL Buffer D+25uL 5x Laemmli buffer with BME and heating for 10 min at room temperature. Beads were removed and samples were boiled at 95ºC for 5-10 minutes to denature proteins for immunoblot analysis.

Proximity Ligation Assay (PLA)

Proximity ligation assay was performed as previously published[35]. Cells were seeded for optimum density according to cell size (MM134 and SUM44PE at 40k/well, MM330 32k/well, CAMA-1 at 20k/well, MCF7 and T47D at 16k/well, HCC1428 at 24k/well) in 10-well chamber coverslides (Greiner Bio-One #543079) and incubated for 48 hours with relevant drug or siRNA (see at 37C at 5% CO2. Cells were washed 2x with room temperature 1x PBS and fixed in 4% paraformaldehyde (Electron Microscopy Sciences #15710) for 15min with shaking at room temperature. Cells were washed 2x with room temperature 1x PBS. Cells were permeabilized with 0.1% Triton X-100 (Fisher BP151-100) in 1x PBS for 15min at room temperature with shaking and rinsed in 1x PBS. PLA was then performed according to Sigma Aldrich Duolink PLA Fluorescence Protocol (DUO92008, DUO92002, DUO92004). Primary antibodies for proteins of interest were diluted to optimal concentration (ER 6F11 1:200; Bethyl MDC1 A300-051A, 1:2500).

dsDNA Quantification (Hoechst Assay)

Cells were plated at optimal density in 96-well plate in 100uL of relevant media (hormone deprived or replete) with appropriate siRNA conditions. 24 hours later, media and any drug treatment were added (100uL together) for a total volume of 100uL in each well. Cells were kept at 37ºC for 6 days, then media was removed, and plate was flash-frozen and stored at -80ºC. For dsDNA quantification, 100uL of TNE buffer (50mM Tris-HCl, 100nM NaCl, 0.1mM EDTA, pH 7.4) was added to each well and plate was incubated at 37ºC for 1 hour. Next, plate

was flash frozen at -80º until all liquid was frozen solid (~45-60min). Plate was thawed completely at room temperature and 100uL of Hoechst 33258 (Thermo Fisher Scientific, #62249) in MiliQ H2O was added to each well for a final concentration 0.1ug/mL Hoechst per well. Fluorescence (360nm ex / 460nm em) was measured on a Bio-Tek Synergy 2 microplate reader.

Quantitative PCR (RT-qPCR)

RNA extractions were performed using the RNeasy Mini kit (Qiagen, Venlo, Netherlands); mRNA was converted to cDNA on an Eppendorf Mastercycler Pro (Eppendorf, Hamburg, Germany) and using Promega reagents: Oligo (dT)15 primer (cat# C110A), Random Primers (cat# C118A), GoScript 5x Reaction Buffer (cat# A500D), 25mM MgCl2 (cat# A351H), 10mM dNTPs (cat# U1511), RNasin Plus RNase Inhibitor (cat# N261B) and GoScript Reverse Transcriptase (cat# A501D). qPCR reactions were performed with PowerUp SYBR Green Master Mix (Life Technologies, cat # 100029284) on a QuantStudio 6 Flex Real-Time PCR system. Expression data were normalized to RPLP0.

The following primers were used: RPLP0, Forward – CAGCATCTACAACCCTGAAG, Reverse – GACAGACACTGGCAACATT; ESR1, Forward – GAAGCTTCGATGATGGGCTTAC, Reverse – CCTGATCATGGAGGGTCAAATC; MDC1, Forward – TACCCAGGCCTTCATGTT, Reverse – GACCTCCCATGGTTCATCTA; TFF1, Forward – GTGCAAATAAGGGCTGCTGTT, Reverse – CAGATCCCTGCAGAAGTGTCTA; PDZK1, Forward – GGTAGACAAAGAGACGGACAAC, Reverse – GACTTCCAGAGAAGTGGGAGTA; PDE4B, Forward – CAAGTTCAGGCGTTCTTCT, Reverse – GTCTGTCCATTGCCGATAC; TFCP2L1, Forward – CCCAAGCTACAATGGTTCTC, Reverse – TCCTGGATCGAAGCTGAT; PTPN1, Forward –

TTCTGTCTGGCTGARACCT, Reverse – CCATCCGAAACTTCCTCATT; IGFBP4, Forward – ACGAGGACCTCTACATCATCC, Reverse – GTCCACACACCAGCACTTG; MYC, Forward – GCTGCTTAGACGCTGGATTT, Reverse – GAGTCGTAGTCGAGGTCATAGT; NRIP1, Forward – GAACTGTTCTCAGGACTCATT, Reverse – TGTCATCCGGAGTCTTCA; PTGES, Forward – AGGATGCCCTGAGACACGGA, Reverse – AGTAGACGAAGCCCAGGAAAAG; DHCR7, Forward – TGCTTCTGTACACGTCTCT, Reverse – GCTTGCAGGCCATTGAT; TUB, Forward – ACAGACTTGTCTCGAGGAG, Reverse – TCTGAGGGTTGACTCCATT; EGLN3, Forward – ATCTGAACAAGAATTGGGATGC, Reverse – ATGGGCTCCACATCTGC; WNT4, Forward – GCCATTGAGGAGTGCCAGTA, Reverse – CCACACCTGCCGAAGAGATG.

RNA Sequencing and Analysis

MM134, MM330, and HCC1428 cells were hormone deprived according to protocol (see above), plated for optimal confluency in 48-well plates, and transfected with 10nM siNT, siMDC1, siER, and siFOXA1 according to the method described above. 24hours after siRNA transfections, 10pM E2 was added. Cells were harvested 24 hours after addition of E2, washed 3x with cold PBS, and frozen at 80C. RNA was extracted as above (see qPCR methods). Knockdown validation via qPCR was performed before sample submission. Biological triplicate samples were analyzed with NovaSEQ 6000 Paired End 150 cycle 2x150 with Poly A Selection and 40 Million Clusters, 80 million Paired End Reads. Analysis of RNA-seq data was performed in conjunction with the University of Colorado Anschutz Medical Campus Bioinformatics Core.

Statistical Considerations

GraphPad Prism 7 was used for all graphical representation and statistical analyses.

REFRENCES

1. U.S. Department of Health and Human Services, C. for D. C. and P. and N. C. I. U.S. Cancer Statistics Working Group. U.S. Cancer Statistics Data Visualizations Tool, based on 2019 submission data (1999-2017). *June 2020*
2. Sikora, M. J., Jankowitz, R. C., Dabbs, D. J. & Oesterreich, S. Invasive lobular carcinoma of the breast: Patient response to systemic endocrine therapy and hormone response in model systems. *Steroids* **78**, 568–575 (2013).
3. Chen, Z. *et al.* Invasive lobular carcinoma of the breast: A special histological type compared with invasive ductal carcinoma. *PLoS One* **12**, 1–17 (2017).
4. Arpino, G., Bardou, V. J., Clark, G. M. & Elledge, R. M. Infiltrating lobular carcinoma of the breast: Tumor characteristics and clinical outcome. *Breast Cancer Res.* **6**, 7–11 (2004).
5. Ciriello, G. *et al.* Comprehensive molecular portraits of invasive lobular breast cancer Giovanni. *Cell* **163**, 506–519 (2016).
6. Smith, C. L. & O'Malley, B. W. Coregulator Function: A Key to Understanding Tissue Specificity of Selective Receptor Modulators. *Endocr. Rev.* **25**, 45–71 (2004).
7. Rakha, E. A. *et al.* Invasive lobular carcinoma of the breast: Response to hormonal therapy and outcomes. *Eur. J. Cancer* **44**, 73–83 (2008).
8. Metzger-Filho, O. *et al.* Relative effectiveness of letrozole compared with tamoxifen for patients with lobular carcinoma in the BIG 1-98 Trial. *J. Clin. Oncol.* **33**, 2772–2778 (2015).
9. Tasdemir, N. *et al.* Comprehensive phenotypic characterization human invasive lobular carcinoma cell lines in 2D and 3D cultures. *Cancer Res.* **78**, 6209–6222 (2018).
10. Mohammed, H. *et al.* Endogenous Purification Reveals GREB1 as a Key Estrogen

Receptor Regulatory Factor. *Cell Rep.* **3**, 342–349 (2013).

11. Theodorou, V., Stark, R., Menon, S. & Carroll, J. S. GATA3 acts upstream of FOXA1 in mediating ESR1 binding by shaping enhancer accessibility. *Genome Res.* **23**, 12–22 (2013).
12. Watters, R. J., Benos, P. V. & Oesterreich, S. To bind or not to bind - FoxA1 determines estrogen receptor action in breast cancer progression. *Breast Cancer Res.* **14**, 1–2 (2012).
13. Hurtado, A., Holmes, K. A., Ross-innes, C. S., Schmidt, D. & Carroll, J. S. FOXA1 is a critical determinant of Estrogen Receptor function and endocrine response Antoni. **43**, 27–33 (2011).
14. Bertucci, F. *et al.* Lobular and ductal carcinomas of the breast have distinct genomic and expression profiles. *Oncogene* **27**, 5359–5372 (2008).
15. Sikora, M. J. *et al.* Invasive lobular carcinoma cell lines are characterized by unique estrogen-mediated gene expression patterns and altered tamoxifen response. *Cancer Res.* **74**, 1463–1474 (2014).
16. Sikora, M. J. *et al.* WNT4 mediates estrogen receptor signaling and endocrine resistance in invasive lobular carcinoma cell lines. *Breast Cancer Res.* **18**, 1–16 (2016).
17. Jung, S. Y., Malovannaya, A., Wei, J., O'Malley, B. W. & Qin, J. Proteomic Analysis of Steady-State Nuclear Hormone Receptor Coactivator Complexes. *Mol. Endocrinol.* **19**, 2451–2465 (2005).
18. Klinge, C. M. Estrogen receptor interaction with co-activators and co-repressors. *Steroids* **65**, 227–251 (2000).
19. McBryan, J. *et al.* Metastatic progression with resistance to aromatase inhibitors is driven by the steroid receptor coactivator SRC-1. *Cancer Res.* **72**, 548–559 (2012).

20. Flach, K. D. *et al.* Endonuclease FEN1 Coregulates ERα Activity and Provides a Novel Drug Interface in Tamoxifen-Resistant Breast Cancer. *Cancer Res.* **80**, 1914–1926 (2020).

21. Zheng, Z. Y. *et al.* Neurofibromin Is an Estrogen Receptor-α Transcriptional Co-repressor in Breast Cancer. *Cancer Cell* **37**, 387-402.e7 (2020).

22. Mohammed, H. *et al.* Rapid immunoprecipitation mass spectrometry of endogenous proteins (RIME) for analysis of chromatin complexes. *Nat. Protoc.* **11**, 316–326 (2016).

23. D'Santos, C., Taylor, C., Carroll, J. S. & Mohammed, H. RIME proteomics of estrogen and progesterone receptors in breast cancer. *Data Br.* **5**, 276–280 (2015).

24. Threonine, C. E., Stewart, G. S., Wang, B., Bignell, C. R. & Taylor, A. M. R. MDC1 is a mediator of the mammalian DNA damage checkpoint. *Nature* **5936**, 5934–5936 (2003).

25. Minter-Dykhouse, K., Ward, I., Huen, M. S. Y., Chen, J. & Lou, Z. Distinct versus overlapping functions of MDC1 and 53BP1 in DNA damage response and tumorigenesis. *J. Cell Biol.* **181**, 727–735 (2008).

26. Goldberg, M. *et al.* MDC1 is required for the intra-S-phase DNA damage checkpoint. *Nature* **421**, 952–956 (2003).

27. Wang, C. *et al.* MDC1 functionally identified as an androgen receptor co-activator participates in suppression of prostate cancer. *Nucleic Acids Res.* **43**, 4893–4908 (2015).

28. Zou, R. *et al.* MDC1 enhances estrogen receptor-mediated transactivation and contributes to breast cancer suppression. *Int. J. Biol. Sci.* **11**, 992–1005 (2015).

29. Szklarczyk, D. *et al.* STRING v11: Protein-protein association networks with increased coverage, supporting functional discovery in genome-wide experimental datasets. *Nucleic Acids Res.* **47**, D607–D613 (2019).

30. Snel, B., Lehmann, G., Bork, P. & Huynen, M. A. String: A web-server to retrieve and

display the repeatedly occurring neighbourhood of a gene. *Nucleic Acids Res.* **28**, 3442–3444 (2000).

31. Fujifilm Wako Chemicals U.S.A. Corporation *et al.* Protein detection using proximity-dependent DNA Ligation Assays. *Nat. Biotechnol.* **20**, 473–477 (2014).

32. Savkur, R. S. & Burris, T. . The coactivator LXXLL nuclear receptor recognition motif. *J. Pept. Res.* **63**, 207–212 (2004).

33. Jungmichel, S. & Stucki, M. MDC1: The art of keeping things in focus. *Chromosoma* **119**, 337–349 (2010).

34. Bernardo, G. M. *et al.* FOXA1 is an essential determinant of ERα expression and mammary ductal morphogenesis. *Development* **137**, 2045–2054 (2010).

35. Goodall, M. L. *et al.* The Autophagy Machinery Controls Cell Death Switching between Apoptosis and Necroptosis. *Dev. Cell* **37**, 337–349 (2016).

36. Sikora, M. J., Johnson, M. D., Lee, A. V. & Oesterreich, S. Endocrine response phenotypes are altered by charcoal-stripped serum variability. *Endocrinology* **157**, 3760–3766 (2016).